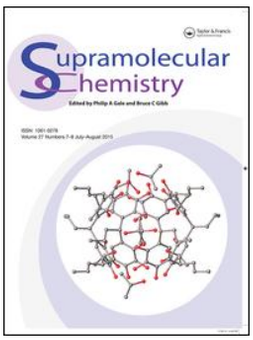

Supramolecular Chemistry

ISSN: 1061-0278 (Print) 1029-0478 (Online) Journal homepage: http://www.tandfonline.com/loi/gsch20

Advantages of organic halogen bonding for halide recognition

Nicholas B. Wageling, George F. Neuhaus, Ariana M. Rose, Daniel A. Decato & Orion B. Berryman

To cite this article: Nicholas B. Wageling, George F. Neuhaus, Ariana M. Rose, Daniel A. Decato & Orion B. Berryman (2015): Advantages of organic halogen bonding for halide recognition, Supramolecular Chemistry, DOI: 10.1080/10610278.2015.1118101

To link to this article: http://dx.doi.org/10.1080/10610278.2015.1118101

SUPRAMOLECULAR CHEMISTRY, 2015
http://dx.doi.org/10.1080/10610278.2015.1118101

Taylor & Francis
Taylor & Francis Group

Advantages of organic halogen bonding for halide recognition

Nicholas B. Wageling[‡], George F. Neuhaus[‡], Ariana M. Rose, Daniel A. Decato and Orion B. Berryman

Department of Chemistry and Biochemistry, University of Montana, Missoula MT, USA

ABSTRACT

The synthesis of a bidentate halogen bonding receptor and a nearly isostructural hydrogen bonding analogue is described. Crystal structures reveal the interactions of each receptor with anions in the solid state, while NMR titrations elucidate bidentate binding and association constants in solution. Of the two, the halogen bonding receptor demonstrates stronger, water resistant halide binding in competitive solvents.

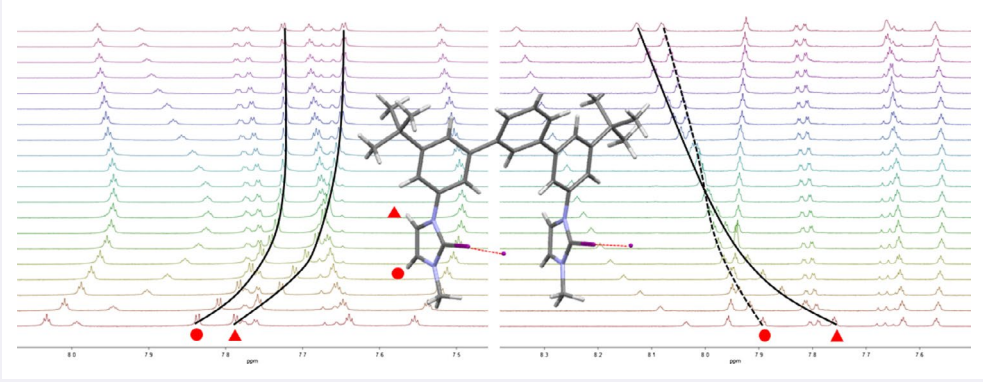

ARTICLE HISTORY
Received 5 October2015
Accepted 24 October2015

KEYWORDS
Halogen bonding; anion recognition; NMR titration

1. Introduction

In the expanding field of anion recognition (*1*), potent receptors have found application in chemical sensing (*2*), anion transport (*3*), ion extraction (*4*), and catalysis (*5*). However, producing tight and selective anion receptors is challenging due to the low charge to radius ratio, pH dependence and high hydration energy of anions as compared to cations (*6*). Furthermore, applications in biological (*7*) and environmental systems necessitate that anion receptors function in competitive, polar and aqueous environments. To overcome these obstacles, an array of strategies are currently employed including: hydrogen bonding (HB) (*8*), electrostatics (*9*), metal-complexation (*10*), and hydrophobic interactions (*11*). In contrast, even though the halogen bond (XB) is a robust noncovalent interaction, it has been relatively under studied in solution.

The stringent linear directionality of the XB (*12*) has been elegantly exploited in receptors to bind anionic guests, including halides (*13*) and oxo-anions (*14*). Because polarisation and charge-transfer contribute to XB interactions, it has been suggested that XB is less susceptible to solvent inhibition than HB (*15*). For example, Hunter recently reported a comparison of inorganic XB and organic HB in a range of solvents.(*15a*) This investigation concluded that HB strength diminished with increasing solvent polarity while the XB remained relatively unperturbed. However, this study contained structurally diverse inorganic XB and organic HB donors (elemental iodine and 4-(phenylazo)phenol). If this trend holds for organic XB donors it would be of great interest due to their structural versatility. Using an imidazolium-based organic XB or HB donor on an identical scaffold provides an opportunity to directly compare organic XB and C–H HB (*16*) in solution. To date, only five experimental investigations (*14b*, *17*) and one computational study (*18*) have compared isostructural imidazolium-based organic XB and HB donors.[1] Herein, we demonstrate that bidentate XB receptor **1** exhibits greater binding affinity for halide guests and maintains stronger interactions in the presence of water than a HB counterpart. These results support that XB is a tractable approach

CONTACT Orion B. Berryman orion.berryman@umontana.edu
[‡]These authors contributed equally.

to anion recognition in competitive biological and environmental systems.

2. Experimental section

2.1. General information

All materials were obtained from commercial sources and used without further purification. NMR spectra were recorded on a 500 or 400 MHz spectrometer. Chemical shifts (δ) are expressed as ppm. For the ^{19}F NMR spectra, C_6F_6 (δ = –164.9 ppm) was used as an internal standard. Signal splitting patterns are indicated as s, singlet; d, doublet; t, triplet; m, multiplet; b, broad. Coupling constants (*J*) are given in Hz. High-resolution mass spectrometry was performed on an electrospray ionization mass spectrometer with a time-of-flight detector.

2.2. General procedure for N-arylation

Salicylaldoxime (0.2 equiv), imidazole (1.2 equiv), Cs_2CO_3 (2.0 equiv), and Cu_2O (0.1 equiv) were added to an oven dried Schlenk tube under an inert atmosphere (dry N_2). A sparged solution of 1-bromo-3-(*tert*-butyl)-5-iodobenzene (**8**) (prepared by a known procedure (*19*)), or 1-bromo-3-iodobenzene **(8a)** (1 equiv, 0.8 M in total reaction mixture) dissolved in dry acetonitrile was then added to the Schlenk tube using a cannula and the clear reaction mixture with Cu_2O and Cs_2CO_3 suspension was raised to 50 °C in an oil bath and left to stir for 25 h. The solution was then allowed to cool to rt before diluting with DCM and filtering through diatomaceous earth. The product was then purified by flash column chromatography using normal phase silica, and/or by vacuum distillation at 1 Torr.

2.3. General procedure for Suzuki–Miyaura cross-coupling

$PdCl_2(PPh_3)_2$ (0.1 equiv), and 1,3-phenylenediboronic acid (0.5 equiv) were added to a Schlenk flask under an inert atmosphere (dry N_2). Sparged solutions of **7**, **7a**, **8** or **8a** in DMF (1 equiv, 0.1 M in total reaction mixture) and TBAF (1 M in THF, 7.8 equiv) were then added to the Schlenk flask with a cannula. The yellow mixture was then heated to 90 °C in an oil bath. The reaction turned black after 10 min, and was allowed to stir at 90 °C under N_2 overnight. After cooling to rt, the volatiles were removed by rotary evaporator leaving a black oil that was dissolved in DCM and filtered through diatomaceous earth. The filtrate was concentrated on rotary evaporator and the resultant black oil was purified by flash column chromatography on normal phase silica.

2.4. General procedure for iodination

6 or **6a** (1 equiv) was dissolved in dry THF and sparged with dry N_2 before cooling to –50 °C. To the slightly yellow mixture, *n*-BuLi (2.5 M in hexanes, 2.5 equiv) was added dropwise, and was allowed to stir at –50 °C for 30 min. A sparged solution of I_2 (0.76 M in THF, 2.3 equiv) was added to the solution dropwise, turning the solution red. The reaction mixture was allowed to warm to rt over 2 h and allowed to stir for an additional 22 h under N_2. The solvent was then removed and the concentrate was dissolved in DCM, washed with saturated aqueous sodium thiosulfate, followed by DI water and finally brine. The organic layer was dried over anhydrous $MgSO_4$, filtered and concentrated. The product was purified by flash column chromatography on normal phase silica.

2.5. General procedure for methylation

4, **4a**, **5**, **5a**, **6** or **6a** (1 equiv) was dissolved in dry DCM and sparged with dry N_2. MeOTf (4 equiv) was then added dropwise to the solution, and it was allowed to stir under N_2 overnight. The product was filtered and purified by recrystallisation.

2.6. General procedure for anion titrations

Stock solutions of **1**, **2** and **3** were prepared in the given solvent. Aliquots (0.500 mL) from each stock solution were transferred via gas-tight syringe into three separate NMR tubes sealed with rubber septa. The stock solutions were then used to make host/guest solutions corresponding to their experiment number. After obtaining free-host spectra of **1**, **2** and **3**, aliquots of corresponding guest solution (containing **1**, **2**, or **3** and TBA^+X^- at specified concentrations) were added to their respective NMR tubes. A spectrum was obtained after each addition. A constant host concentration was maintained, while TBA^+X^- concentrations in the NMR tube gradually increased throughout the titration (see data in SI). HypNMR 2008 (*20*) was used to fit the binding isotherms for multiple signals (**1**: H_a, H_b, and H_c; **2**: H_a, H_b, H_c, H_d, H_e, H_f, and H_g; **3**: H_a, H_b, H_c, and H_d) simultaneously.

2.6.1. 1-(3-bromo-5-(tert-butyl)phenyl)-1H-imidazole (7)

Prepared from **8** by following the general procedure for *N*-arylation. Yellow oil: 85.7% yield; eluent conditions 1.5% (v/v) NH_4OH (14.8 M, aq.) 3:2 hexanes:EtOAc; ^1H NMR (500 MHz, $CDCl_3$) δ 7.83 (s, 1H), 7.52 (t, J = 1.6 Hz, 1H), 7.37 (t, J = 1.9 Hz, 1H), 7.31 (t, J = 1.7 Hz, 1H), 7.26 (s, 1H), 7.21 (s, 1H), 1.35 (s, 9H). $^{13}C[^1H]$ NMR (125 MHz, $CDCl_3$) δ 155.39, 138.22, 135.60, 130.60, 127.93, 123.10, 121.96, 118.28, 117.64, 35.17, 31.07. HRMS (ESI-TOF) *m/z*: 279.0491 $(M + 1H)^+$ 50%, 281.0472 $(M + 2 + 1H)^+$ 50%, $C_{13}H_{15}BrN_2$ (calc. 278.04).

2.6.2. 1-(3-bromophenyl)-1H-imidazole (7a)

Prepared from **8a** by following the general procedure for *N*-arylation. Yellow oil: 84% yield; bp: 190–200 °C, ~1 Torr. ^{1}H NMR (500 MHz, $CDCl_3$) δ = 7.86 (s, 1H), 7.56 (t, J = 2.0 Hz, 1H), 7.51–7.49 (m, 1H), 7.37–7.32 (m, 2H), 7.27 (s, 1H), 7.22 (s, 1H). ^{13}C[^{1}H] NMR (125 MHz, $CDCl_3$) δ = 138.5, 135.6, 131.3, 130.9, 130.7, 124.7, 123.5, 120.1, 118.2. HRMS (ESI-TOF) *m/z*: 222.9865 $(M + 1H)^+$ 50%, 224.9845 $(M + 2 + 1H)^+$ 50%, $C_9H_7BrN_2$ (calc. 221.98).

2.6.3. 1,1′-(5,5″-di-tert-butyl-[1,1′:3′,1″-terphenyl]-3,3″-diyl)bis(1H-imidazole) (6)

Prepared from **7** by following the general procedure for Suzuki–Miyaura cross-coupling. White solid: 60% yield; eluent conditions 0.25% (v/v) MeOH, 1.5% (v/v) NH_4OH (14.8 M, aq.) in EtOAc; mp: 207–210 °C. ^{1}H NMR (400 MHz, DMSO-d_6) δ 8.39 (d, J = 1.4 Hz, 2H), 8.06 (t, J = 1.8 Hz, 1H), 7.90 (t, J = 1.3 Hz, 2H), 7.82–7.76 (m, 4H), 7.68 (t, J = 1.5 Hz, 2H), 7.64–7.59 (m, 3H), 7.12 (d, J = 1.3 Hz, 2H), 1.41 (s, 18H). ^{13}C[^{1}H] NMR (100 MHz, DMSO-d_6) δ 153.50, 141.81, 140.71, 137.43, 135.91, 129.70, 129.46, 126.83, 126.26, 122.60, 118.46, 116.80, 116.73, 34.98, 31.05. HRMS (ESI-TOF) *m/z*: 238.1465 $(M + 2H)^{2+}$, $C_{32}H_{34}N_4$ (calc. 474.28).

2.6.4. 3,3″-di(1H-imidazol-1-yl)-1,1′:3′,1″-terphenyl (6a)

Prepared from **7a** by following the general procedure for Suzuki–Miyaura cross-coupling. Yellow oil: 78% yield; eluent conditions 2.5% (v/v) MeOH, 1.5% (v/v) NH_4OH (14.8 M, aq.) in EtOAc. ^{1}H NMR (400 MHz, $CDCl_3$) δ = 7.95 (s, 2H), 7.81 (t, J = 2.5 Hz, 1H), 7.66–7.64 (m, 6H), 7.62–7.57 (m, 3H), 7.42 (dt, J = 9.5 Hz, 2.0 Hz, 2H), 7.36 (s, 2H), 7.25 (s, 2H). ^{13}C[^{1}H] NMR (100 MHz, $CDCl_3$) δ = 143.1, 140.9, 138.1, 135.8, 130.62, 130.58, 129.9, 127.1, 126.6, 126.3, 120.8, 120.6, 118.5. HRMS (ESI-TOF) *m/z*: 363.1604 $(M + 1H)^+$ $C_{24}H_{18}N_4$ (calc. 362.15)

2.6.5. 1,1′-(5,5″-di-tert-butyl-[1,1′:3′,1″-terphenyl]-3,3″-diyl)bis(2-iodo-1H-imidazole) (4)

Prepared from **6** by following the general procedure for iodination. White solid: 58% yield; eluent conditions 1.5% (v/v) NH_4OH (14.8 M, aq.) 3:2 hexanes:EtOAc (note: product degrades on normal phase silica); mp: 157 °C (decomposition). ^{1}H NMR (500 MHz, CD_3CN) δ 8.01 (t, J = 1.6 Hz, 1H), 7.89 (t, J = 1.6 Hz, 2H), 7.76 (dd, J = 7.7, 1.7 Hz, 2H), 7.64–7.59 (m, 3H), 7.50 (t, J = 1.8 Hz, 2H), 7.45 (d, J = 1.2 Hz, 2H), 7.16 (d, J = 1.1 Hz, 2H), 1.42 (s, 18H). ^{13}C[^{1}H] NMR (125 MHz, CD_3CN) δ 154.48, 142.53, 141.73, 139.81, 133.31, 130.70, 127.88, 127.10, 126.24, 125.64, 124.34, 123.66, 91.53, 35.94, 31.42. HRMS (ESI-TOF) *m/z*: 364.0431 $(M + 2H)^{2+}$, $C_{32}H_{32}I_2N_4$ (calc. 726.07).

2.6.6. 3,3″-bis(2-iodo-1H-imidazol-1-yl)-1,1′:3′,1″-terphenyl (4a)

Prepared from **6a** by following the general procedure for iodination. White solid: 52% yield; eluent conditions 1.5% (v/v) NH_4OH (14.8 M, aq.) 1:1 hexanes:acetone. ^{1}H NMR (500 MHz, CD_2Cl_2) δ = 7.89 (s, 1H), 7.81 (d, J = 7.8 Hz, 2H), 7.70–7.67 (m, 4H), 7.63–7.59 (m, 3H), 7.39 (d, J = 7.9 Hz, 2H), 7.32 (d, J = 1.3 Hz, 2H), 7.19 (d, J = 1.2 Hz, 2H). ^{13}C[^{1}H] NMR (100 MHz, $CDCl_3$) δ = 142.43, 140.56, 139.11, 133.22, 130.05, 129.93, 127.97, 127.09, 126.25, 125.84, 125.75, 124.93, 90.42 HRMS (ESI-TOF) *m/z*: 307.9805 $(M + 2H)^{2+}$ $C_{24}H_{16}I_2N_4$ (calc. 613.94).

2.6.7. 1-(3″,5-di-tert-butyl-5″-(1H-imidazol-1-yl)-[1,1′:3′,1″-terphenyl]-3-yl)-2-iodo-1H-imidazole (5)

Prepared from **4** by following the general iodination procedure (monoiodination occurs as a side product in the iodination step). White solid: 17% yield; eluent conditions 1.5% (v/v) NH_4OH (14.8 M, aq.) 2:3 hexanes:EtOAc; mp: 140 °C (decomposition). ^{1}H NMR (400 MHz, CD_3CN) δ 8.05 (s, 1H), 8.03 (t, J = 1.7 Hz, 1H), 7.89 (t, J = 1.7 Hz, 1H), 7.79–7.74 (m, 3H), 7.69 (t, J = 1.8 Hz, 1H), 7.64–7.57 (m, 3H), 7.55 (t, J = 1.9 Hz, 1H), 7.50 (t, J = 1.8 Hz, 1H), 7.46 (d, J = 1.3 Hz, 1H), 7.16 (d, J = 1.3 Hz, 1H), 7.13 (s, 1H), 1.43 (s, 18H). ^{13}C[^{1}H] NMR (125 MHz, CD_3CN) δ 155.03, 154.42, 143.10, 142.56, 142.04, 141.66, 139.75, 138.81, 133.28, 130.58, 127.96, 127.82, 127.18, 126.22, 125.65, 124.31, 124.22, 123.65, 91.54, 35.91, 31.39, 31.36. HRMS (ESI-TOF) *m/z*: 301.0948 $(M + 2H)^{2+}$, $C_{32}H_{33}IN_4$ (calc. 600.17).

2.6.8. 1,1′-(5,5″-di-tert-butyl-[1,1′:3′,1″-terphenyl]-3,3″-diyl)bis(2-iodo-3-methyl-1H-imidazol-3-ium) trifluoromethanesulfonate (1)

Prepared from **4** by following the general procedure for methylation. White solid: 72% yield; Recrystallized from $CHCl_3$; mp: 218 °C (decomposition). ^{1}H NMR (500 MHz, CD_3CN) δ 8.03 (t, J = 1.6 Hz, 2H), 7.99 (t, J = 1.6 Hz, 1H), 7.83 (d, J = 2.1 Hz, 2H), 7.77 (dd, J = 7.6, 1.9 Hz, 4H), 7.68–7.63 (m, 3H), 7.55 (t, J = 1.8 Hz, 2H), 3.93 (s, 6H), 1.44 (s, 18H). ^{13}C[^{1}H] NMR (100 MHz, CD_3CN) δ 155.40, 143.17, 141.21, 138.31, 130.97, 128.27, 127.73, 127.68, 127.57, 127.04, 124.16, 123.45, 121.99 (q, J = 318 Hz), 101.78, 40.76, 36.12, 31.32. ^{19}F NMR (376 MHz, CD_3CN) δ –79.70. HRMS (ESI-TOF) *m/z*: 378.0587 M^{2+}, $C_{34}H_{38}I_2N_4^{2+}$ (calc. 756.12, triflate anions omitted).

2.6.9. 1,1′-([1,1′:3′,1″-terphenyl]-3,3″-diyl) bis(2-iodo-3-methyl-1H-imidazol-3-ium) trifluoromethanesulfonate (1a)

Prepared from **4a** by following the general procedure for methylation. White solid: 86% yield; filtered from reaction and rinsed with DCM to give product. ^{1}H NMR (400 MHz, CD_3CN) δ 8.26 (s, 2H), 8.16–8.11 (m, 7H), 7.87–7.81 (m,

4H), 7.73–7.66 (m, 3H), 4.13 (s, 6H) $^{13}C[^1H]$ NMR (125 MHz, CD_3CN) δ 143.29, 140.63, 138.42, 131.65, 131.10, 130.68, 128.13, 127.78, 127.57, 126.84, 126.65, 126.33, 123.28, 120.73, 101.78, 40.73 (note: the peaks at 123.28 and 120.73 are from ^{19}F coupling to the triflate carbon. The carbon peak should split into a quartet, but only the two inside peaks are observed, as the two outside peaks are below the noise) ^{19}F NMR (470 MHz, CD_3CN) δ 79.68 HRMS (ESI-TOF) *m/z*: 321.9961 M^{2+}, $C_{26}H_{22}I_2N_4^{2+}$ (calc. 643.99, triflate anions omitted)

2.6.10. 1-(3″,5-di-tert-butyl-5″-(3-methyl-1H-imidazol-3-ium-1-yl)-[1,1′:3′,1″-terphenyl]-3-yl)-2-iodo-3-methyl-1H-imidazol-3-ium trifluoromethanesulfonate (2)

Prepared from **5** by following the general procedure for methylation. White solid: 86% yield; recrystallized from 1:9 hexanes:$CHCl_3$; mp 146 °C (decomposition). ^1H NMR (500 MHz, CD_3CN) δ 9.00 (s, 1H), 8.04 (t, *J* = 1.6 Hz, 1H), 8.02 (t, *J* = 1.5 Hz, 1H), 7.96 (t, *J* = 1.6 Hz, 1H), 7.88 (t, *J* = 1.9 Hz, 1H), 7.84 (d, *J* = 2.1 Hz, 1H), 7.81–7.75 (m, 4H), 7.68–7.64 (m, 2H), 7.63 (t, *J* = 1.9 Hz, 1H), 7.56 (t, *J* = 1.8 Hz, 2H), 3.96 (s, 3H), 3.93 (s, 3H), 1.44 (d, *J* = 2.9 Hz, 18H). $^{13}C[^1H]$ NMR (125 MHz, CD_3CN) δ 155.77, 155.37, 143.48, 143.19, 141.33, 141.12, 138.20, 136.48, 136.47, 136.25, 130.89, 128.36, 128.26, 127.75, 127.69, 127.58, 127.15, 127.03, 125.18, 124.13, 123.39, 122.70, 119.74, 119.48, 101.70, 40.75, 37.20, 36.12, 36.10, 31.26, 31.24. ^{19}F NMR (376 MHz, CD_3CN) δ -79.69. HRMS (ESI-TOF) *m/z*: 315.1095 M^{2+}, $C_{34}H_{39}IN_4^{2+}$ (calc. 630.22, triflate anions omitted).

2.6.11. 1,1′-(5,5″-di-tert-butyl-[1,1′:3′,1″-terphenyl]-3,3″-diyl)bis(3-methyl-1H-imidazol-3-ium) trifluoromethanesulfonate (3)

Prepared from **6** using the general procedure for methylation. White solid: 96% yield; recrystallized from 1:3 hexanes:$CHCl_3$; mp: 203 °C (decomposition). ^1H NMR (400 MHz, CD_2Cl_2) δ 9.56 (s, 2H), 8.11 (s, 1H), 8.00–7.98 (t, 2H), 7.88 (s, 2H), 7.75–7.69 (m, 4H), 7.65–7.61 (t, 1H), 7.46 (t, *J* = 1.6 Hz, 2H), 7.45–7.42 (t, 2H), 4.12 (s, 6H), 1.44 (s, 18H). $^{13}C[^1H]$ NMR (125 MHz, CD_2Cl_2) δ 155.36, 143.56, 140.84, 136.82, 135.67, 130.10, 127.62, 127.15, 126.88, 124.51, 122.08, 119.40, 118.59, 54.00, 37.30, 35.82, 31.47. ^{19}F NMR (376 MHz, CD_2Cl_2) δ -81.36. HRMS (ESI-TOF) *m/z*: 252.1621 M^{2+}, $C_{34}H_{40}N_4^{2+}$ (calc. 504.32, triflate anions omitted)

3. Results and discussion

Bidentate XB scaffold **1** and controls **2** and **3** were prepared by regioselective *N*-arylation (*21*) of **8** with imidazole followed by a twofold palladium catalysed Suzuki–Miyaura cross-coupling (*22*) (Scheme 1). The conformational

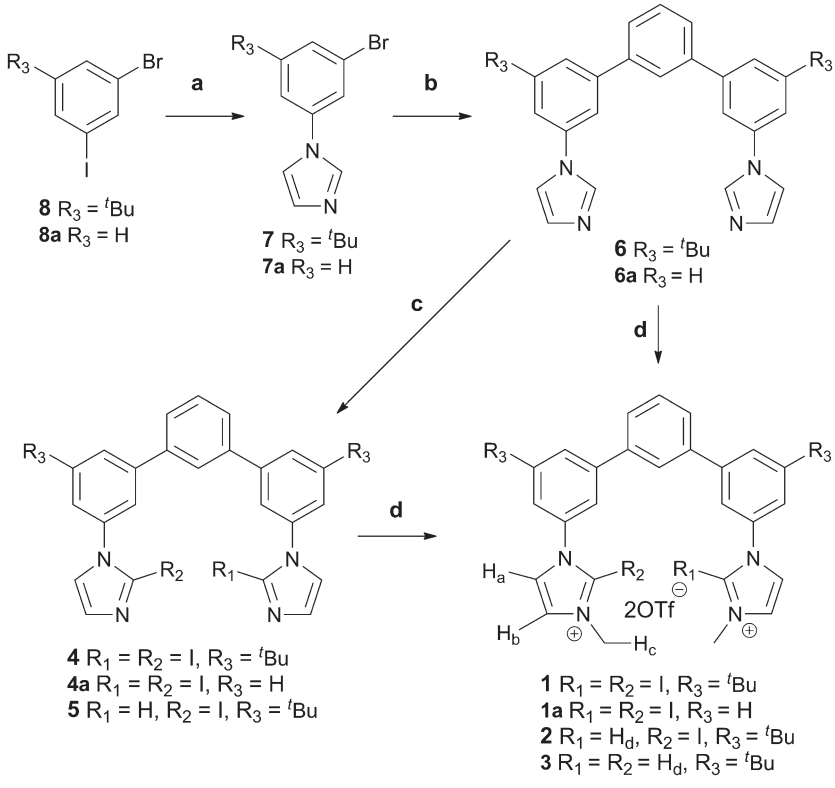

Scheme 1. (a) Imidazole (1 equiv), Cu_2O (10 mol%), Saldox (20 mol%), Cs_2CO_3 (2 equiv), MeCN, 50 °C, 18 h, 86%; (b) 1,3-phenylenediboronic acid (0.5 equiv), $PdCl_2(PPh_3)_2$ (10 mol%), TBAF/THF (2.5 M, 4 equiv), DMF, 90 °C, 72 h, 60%; (c) 1) *n*-BuLi (2.6 equiv), THF, –78 °C, 30 min 2) I_2/THF (2.7 equiv), –78 °C→rt, 24 h, **4** 58%, **5** 17%; (d) MeOTf (4.2 equiv), DCM, rt, 24 h, **1** 72%, **2** 86%, **3** 96%.

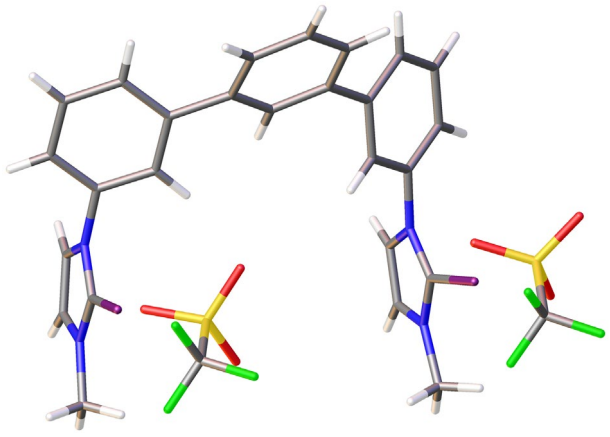

Figure 1. (Colour online) Crystal structure of **1a** highlighting the linear XB between the iodines (purple) and triflate oxygens.

flexibility of the *meta*-terphenyl scaffold allows for bidentate binding while taking advantage of the stringent directional requirements of XB. To create the XB receptor **1**, the imidazole C2 carbons of **6** were deprotonated with *n*-BuLi and the reaction was quenched with elemental iodine, generating **4** in 58% yield. The monoiodinated scaffold **5**, which serves as a convenient control after alkylation, was separated from **4** via flash column chromatography in 17% yield. Scaffolds **4**, **5** and **6** were then alkylated with methyl triflate to produce the activated dicationic XB receptors **1** and **2**, and the control HB receptor **3**, respectively.

To grow suitable crystals for X-ray diffraction, a less soluble non-*tert*-butyl analogue **1a** (Figure 1) was employed. Diffraction quality crystals of **1a** were formed by slow evaporation of an acetone solution. Scaffold **1a** crystallizes in the $P\bar{1}$ space group with two molecules per unit cell. **1a** is preorganised in the solid state with both iodines directed to the same side of the molecule. **1a** exhibits strong XB to the triflate counter anions as indicated by the close I···O contacts (2.825(2) Å and 2.810(2) Å, 79.3% and 78.9% of the sums of the van der Waals radii, Σr_{vdW}, respectively) (*23*) and near linear arrangement of C–I···O ∠ (169.73(1)° and 171.86(9)°). Additionally, there are anion–heteroarene interactions (*24*) contributing to crystal formation: each triflate counteranion lies between two electron-deficient imidazolium rings, forming contacts between the triflate oxygen and the methylated nitrogen of the imidazolium. Crystal packing reveals alternating layers of XB receptors where the donor iodines from each layer are directed towards each other forming a linear array of iodines throughout the crystal (SI Figure S1). The counteranions interpenetrate each layer forming ion pairing interactions and XB that stitch together neighbouring layers.

In contrast, *tert*-butyl substituted HB receptor **3** adopts a splayed out conformation in the solid state (Figure 2). X-ray diffraction quality crystals were grown by vapour diffusion of THF into MeCN solution. **3** crystallizes in the $P\bar{1}$ space group with two molecules per unit cell. The receptor interacts with the triflate anions through one moderate HB and multiple anion–heteroarene contacts. The lack of preorganisation of **3** in the solid state may arise from the relaxed linearity requirements of HB as compared to XB. Moderate HB is observed between an imidazolium C2 hydrogen (H_d) and one triflate (C–H···O ∠166.0954(12)° and C–H···O distance of 2.25831(16) Å). The other triflate molecule interacts via weak anion–heteroarene contacts with the electron-deficient imidazolium rings (C2···O 3.1431(2) Å). Additionally, one of the triflate fluorines is directed at a peripheral aryl C–H hydrogen (*25*).

To investigate the strength of XB in solution, ^{1}H NMR titrations were performed with each receptor and tetra-*n*-butylammonium (TBA) halides. Initial titrations were run in 1:1 CD_2Cl_2:$CDCl_3$. However, these conditions with **1** produced association constants that were beyond the detection limit of the NMR spectrometer (>10^5 M^{-1}) (*26*). To address this limitation, subsequent titrations were performed in CD_3CN wetted with 1% D_2O (v/v) at 289 K.[2]

Association constants were obtained by simultaneously fitting the most responsive proton signals (**1**: H_a, H_b, and H_c; **2**:[3] H_a, H_b, H_c, and H_d; **3**: H_a, H_b, H_c, and H_d) to the stepwise association model described below. The presence of

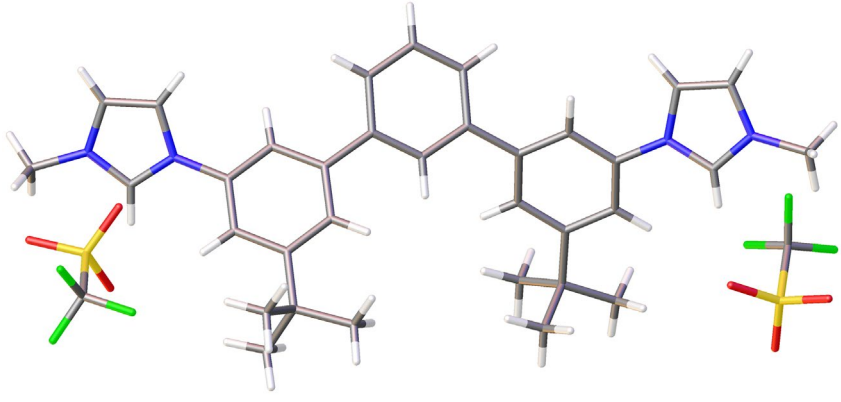

Figure 2. (Colour online) Crystal structure of HB receptor **3**, with a non-convergent conformation.

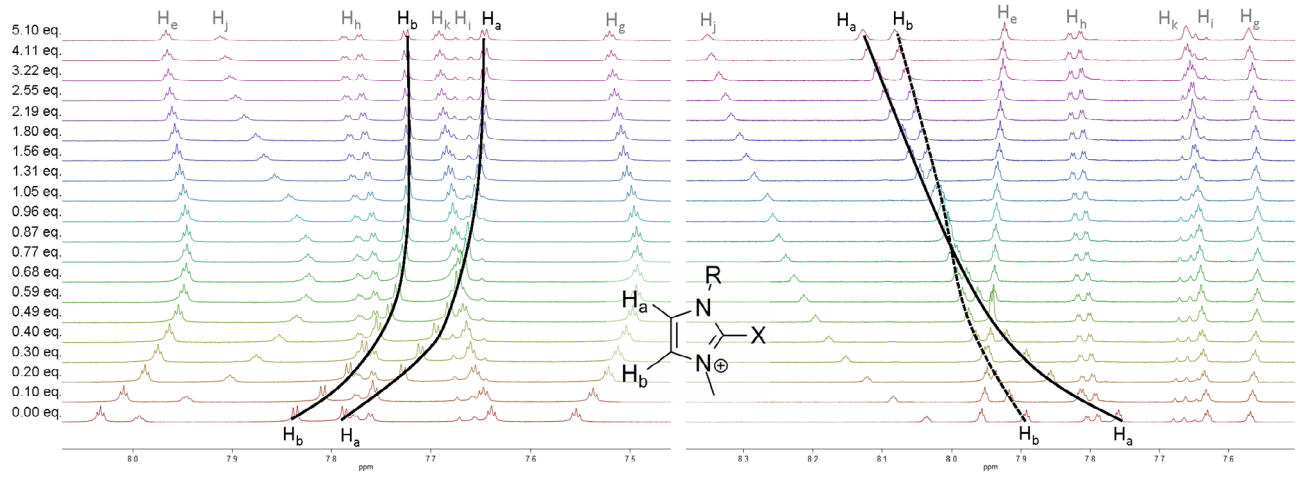

Figure 3. (Colour online) ^{1}H NMR spectra of XB receptor **1** (left) and HB receptor **3** (right) titrated with TBACl and TBABr, respectively (both titrations performed in 1% D_2O in CD_3CN).

Table 1. Anion association constants in mixed solvents.

Host	Anion[a]	Solvent	K_1 [b]	K_2 [b]
1	Cl^-	CD_3CN 1% D_2O	37,700	432
	Br^-	CD_3CN 1% D_2O	28,900	356
	I^-	CD_3CN 1% D_2O	12,990	455
	Br^-	CD_3CN	236,000	2 380
	Br^-	CD_3CN 5% D_2O	3410	293
2	Cl^-	CD_3CN 1% D_2O	5902	59.2
3	Cl^-	CD_3CN 1% D_2O	935	57.0
	Br^-	CD_3CN 1% D_2O	759	64.0
	I^-	CD_3CN 1% D_2O	624.3	47.3
	Br^-	CD_3CN	11,000	425
	Br^-	CD_3CN 5% D_2O	229	18.4

Note: All mixed solvents are v/v. Each titration was performed at 289 K to encourage intramolecular interactions, and discourage degradation of the receptor with iodide.
[a]All anions used were tetrabutylammonium salts.
[b]Calculated based on imidazolium and methyl protons. Errors estimated to be 10%.

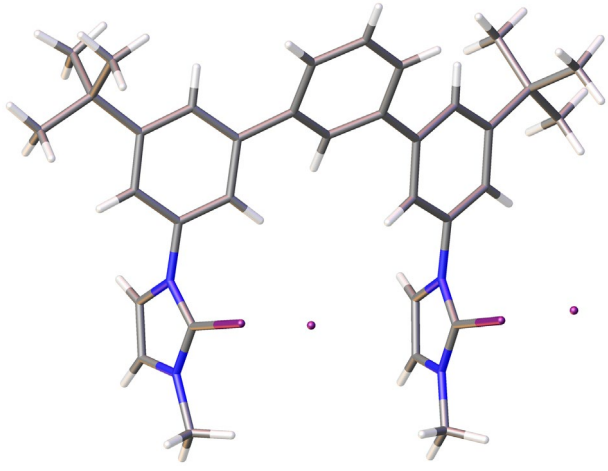

Figure 4. (Colour online) Crystal Structure of **1**·2I^- highlighting strong XB to iodide.

two different binding events is supported by the significant change in direction or the cessation of chemical shift perturbation after one equivalent of guest is added. Based on the dicationic design of the molecule, it was hypothesised that the most significant and plausible binding modes would be 2:1, 1:1 and 1:2 receptor:guest associations. An exhaustive search of binding modes showed that the data did not fit a stepwise 2:1 receptor:guest association model. The dicationic nature of the receptor and the statistical results from fitting the binding isotherms indicate that 1:1 and 1:2 receptor:guest associations are the dominant species in solution. This, along with lack of 2:1 association in the solid state, led to the rejection of the stepwise 2:1 association model. Strong XB in solution is indicated by the halide induced upfield shifts (*14b*, *27*) of the imidazolium protons in **1** (Figure 3). In stark contrast, the analogous imidazolium protons of **3** shifted downfield throughout the titrations, as expected for HB. To further highlight the spectroscopic difference between XB and HB in solution, TBACl was titrated into monoiodinated receptor **2**. The protons on the iodinated imidazolium initially shifted upfield while the protons on the non-iodinated

imidazolium (HB) shifted downfield, suggestive of both XB and HB, respectively, in solution (SI Figure S2).

In these competitive conditions, receptor **1** exhibited significant association constants (Table 1). The trend in halide binding follows the Hofmeister series (Cl^- $K_1 = 37{,}700\ M^{-1}$; Br^- $K_1 = 28{,}900\ M^{-1}$; and I^- $K_1 = 12{,}990\ M^{-1}$), with all values 24–40 times larger than the HB receptor **3**. The trend with **3** also followed the Hofmeister series, suggesting that the difference in binding between **1** and **3** is not due to size exclusion of the anion. Receptor **2**, which can only form one XB, showed an intermediate association to chloride ($K_1 = 5902\ M^{-1}$).

To explore solvent effects, receptors **1** and **3** were additionally titrated with TBABr in neat CD_3CN and 5% D_2O:CD_3CN. The logarithms of the overall equilibrium constants (log [K_1K_2]) of each titration were compared. HB receptor **3** showed a 46% reduction in binding strength from 0 to 5% D_2O, while XB **1** showed only a 32% reduction in binding strength.[4] These data further demonstrate that **1** is less affected by water, highlighting the solvent resistance of organic XB.

Both receptors **1** and **3** form bidentate interactions with halides in solution as evidenced by comparing K_1 and K_2. The K_2 values for **1** are two orders of magnitude lower than the corresponding K_1 values, suggesting that for the 1:1 interaction, the receptor binds in a bidentate fashion. The same trend is observed for **3**. If monodentate binding were dominant, it is likely for this system that the magnitude of K_2 would be similar to K_1. Further support of bidentate binding is found by comparing the chloride titrations of **1** and **2**. The K_1 values of **1** and **2** are an order of magnitude apart, which can be partially explained by the ability of **1** to form a second XB. Bidentate XB is supported as the dominant conformation in solution and is responsible for the strong association of **1** with halides in competitive organic/aqueous environments.

Despite numerous attempts, **1**·2I^- was the only halide salt for which X-ray quality crystals were obtained (Figure 4). Small colourless plates developed upon slow evaporation of a 1% D_2O:CD_3CN solution. The receptor crystallises into the *P*21/c space group with 12 molecules in the asymmetric unit cell. Even though **1**·2I^- contains bulky *tert*-butyl groups, similarities to **1a** are observed in the solid state. Strong monodentate XB to both counter anions is present ($I\cdots I^-$ distances of 3.314 to 3.406 Å, 81 to 83% Σr_{vdW}, ∠ 170.72° to 177.97°). Two distinct receptor conformations are observed in the crystal. In one, iodide counter anions are sandwiched between the imidazolium rings of an adjacent scaffold, forming anion–heteroarene contacts ($C2\cdots I^-$, 3.708(5) Å). The other conformation has the iodoimidazoliums perpendicular to each other. These two conformations form separate columns, of which single planes orthogonal to the columns create a checkerboard packing motif of alternating conformations (see SI Figure S3). While monodentate XB is observed in both solid state crystal structures of the XB receptor, solution data suggests bidentate interactions are the dominant binding mode in solution.

To further investigate the bidentate conformation, DFT calculations were performed (*28*). Energy minimisations were executed at the B98 level of theory, using the 6-31+G(d,p) basis set for non-halogen atoms and LANL2DZ with effective core potential for all halogens. The iodine atoms were further augmented with diffuse functions of p-symmetry and polarisation functions of d-symmetry. This basis set has been shown to correlate well with experimental halogen bonding studies (*14a*). Three conformations[5] were studied for both **1** and **3**: a bidentate binding conformation, a monodentate binding conformation and an unbound conformation. The starting points for each calculation were informed by the crystal structures of **1**, **1a** and **3** as well as from the rational design of the compounds. Each analysed structure was confirmed as minima on the potential energy surfaces. Bidentate XB to chloride resulted in the greatest stabilisation for **1** as compared to the unbound mode ($\Delta G = -23.66$ kcal mol^{-1}) followed by monodentate binding ($\Delta G = -9.19$ kcal mol^{-1}). In each case, the $C–I\cdots Cl^-$ distances and angles represented significant XB; the $C–I\cdots Cl^-$ distances were less than 80% of the Σr_{vdW}, and the angles were all above 169°. The HB receptor **3** showed the same trend with bidentate binding being the most stable vs. the unbound state ($\Delta G = -21.27$ kcal mol^{-1}) followed by monodentate binding ($\Delta G = -14.83$ kcal mol^{-1}). These computations add further evidence in favour of bidentate binding for both the XB and HB receptors described here.

4. Conclusions

With experimental evidence of XB in two phases, and computational data that supports favourable bidentate binding in the gas phase, this research demonstrates the advantages of XB donors over C–H HB donors on imidazolium hosts. Crystal structures displayed strong XB with triflate and iodide counter anions with the XB donors directed towards the same side of the molecule. Solution studies demonstrated that in this system XB outcompetes C–H HB for halide recognition. Furthermore, the greater resistance of organic XB to aqueous solvents was highlighted from titrations in different solvent mixtures. The growing need for anion receptors to function in competitive situations underscores the importance of fully understanding these noncovalent interactions. This example of a XB anion receptor is evidence that organic XB is a tractable design principle that can be used to overcome competitive environments.

Supplemental material

Spectral data (^{1}H, ^{13}C, and ^{19}F NMR) of all new compounds, titration data and the CIF information of **1a**, 1·2I^- and 3. This material is available online here: http://dx.doi.org/10.1080/10610278.2015.1118101.

Notes

1. Of the experimental studies, only two have looked at binding in partially aqueous solvent. To date, our report is the only study that we know of that quantifies the effect of water on the halide binding of these haloimidazolium receptors.
2. 289 K was chosen to encourage intermolecular interactions, and eliminate degradation of **1** with TBA^+I^-.
3. For asymmetric receptor **2**, protons H_e, H_f, and H_g were also followed. See general titration section of the SI.
4. The difference between the logarithms of the overall association constants for the 0% D_2O and the 5% D_2O systems was divided by the value for the 0% system, and multiplied by 100 to give the per cent difference. The values for the logarithms of the overall association constant are the averages of the three titrations performed in that solvent system. The error in each titration is estimated at 10%.
5. The conformations used were at energetic minima. Although this was not an exhaustive search of binding conformations, the rational design of the compounds (along with crystal structures of **1**, **1a**, and **3**) was used as starting points for the DFT calculations.

Acknowledgements

We would like to acknowledge A. C. Sather for collecting preliminary data for the crystal structure in Figure 1, the UM CBSD X-ray core for all other crystal structures, and the CBSD NMR core for support of the NMR spectrometers.

Funding

This work was financially supported by the Center for Biomolecular Structure and Dynamics CoBRE [grant number NIGMS P20GM103546]; National Science Foundation (NSF)-MRI [grant number CHE – 1337908]; Montana University System MREDI [grant number 51030-MUSRI2015-02] and the University of Montana (UM). Funding for N. W. was provided by the UM CBSD Fellowship programme (NIGMS P20GM103546).

References

(1) Busschaert, N.; Caltagirone, C.; Rossom, W.V.; Gale, P.A. *Chem. Rev.* **2015**, *115*, 8038–8155.
(2) Evans, N.H.; Beer, P.D. *Angew. Chem. Int. Ed.* **2014**, *53,* 11716–11754.
(3) Brotherhood, P.R.; Davis, A.P. *Chem. Soc. Rev.* **2010**, *39,* 3633–3647.
(4) Kim, S.K.; Sessler, J.L. *Acc. Chem. Res.* **2014**, *47,* 2525–2536.
(5) Zhang, Z.; Schreiner, P. R. *Chem. Soc. Rev.* **2009**, *38,* 1187–1198.
(6) Schneider, H.-J.; Yatsimirsky, A. *Principles and Methods in Supramolecular Chemistry*; Wiley: Chichester, 1999; Bianchi, A.; Bowman-James, K.; Garcia-Espana, E. *Supramolecular Chemistry of Anions*; Wiley-VCH: New York, 1997.
(7) Scholfield, M.R.; Zanden, C.M.V.; Carter, M.; Ho, P.S. *Protein Sci.* **2013**, *22,* 139–152.
(8) Kubik, S. *Chem. Soc. Rev.* **2010**, *39,* 3648–3663.
(9) Llinares, J.M.; Powell, D.; Bowman-James, K. *Coord. Chem. Rev.* **2003**, *240,* 57–75.
(10) Mateus, P.; Lima, L.M.P.; Delgado, R. *Polyhedron* **2013**, *52,* 25–42.
(11) Hua, Y.; Liu, Y.; Chen, C.-H.; Flood, A.H. *J. Am. Chem. Soc.* **2013**, *135,* 14401–14412.
(12) Mukherjee, A.; Tothadi, S.; Desiraju, G.R. *Acc. Chem. Res.* **2014**, *47,* 2514–2524; Legon, A.C. *Phys. Chem. Chem. Phys.* **2010**, *12,* 7736–7747; Arman, H.D.; Gieseking, R.L.; Hanks, T.W.; Pennington, W.T. *Chem. Commun.* **2010**, *46,* 1854–1856; Aakeroy, C.B.; Champness, N.R.; Janiak, C. *CrystEngComm* **2010**, *12,* 22–43; Metrangolo, P.; Meyer, F.; Pilati, T.; Resnati, G.; Terraneo, G. *Angew. Chem. Int. Ed.* **2008**, *47,* 6114–6127; Politzer, P.; Lane, P.; Concha, M.C.; Ma, Y.; Murray, J.S. *J. Mol. Model.* **2007**, *13,* 305–311.
(13) Mullaney, B.R.; Thompson, A.L.; Beer, P.D. *Angew. Chem. Int. Ed.* **2014**, *53,* 11458–11462.
(14) Chudzinski, M.G.; Taylor, M.S. *J. Org. Chem.* **2012**, *77,* 3483–3491; Cametti, M.; Raatikainen, K.; Metrangolo, P.; Pilati, T.; Terraneo, G.; Resnati, G. *Org. Biomol. Chem.* **2012**, *10,* 1329–1333.
(15) Robertson, C.C.; Perutz, R.N.; Brammer, L.; Hunter, C.A. *Chem. Sci.* **2014**, *5,* 4179–4183; Langton, M.J.; Robinson, S.W.; Marques, I.; Felix, V.; Beer, P.D. *Nat. Chem.* **2014**, *6,* 1039–1043.
(16) Hua, Y.; Flood, A.H. *Chem. Soc. Rev.* **2010**, *39,* 1262–1271.
(17) Tepper, R.; Schulze, B.; Jäger, M.; Friebe, C.; Scharf, D.H.; Görls, H.; Schubert, U.S. *J. Org. Chem.* **2015**, *80,* 3139–3150; Zapata, F.; Caballero, A.; White, N.G.; Claridge, T.D.W.; Costa, P.J.; Félix, V.t.; Beer, P.D. *J. Am. Chem. Soc.* **2012**, *134,* 11533–11541; Walter, S.M.; Kniep, F.; Rout, L.; Schmidtchen, F.P.; Herdtweck, E.; Huber, S.M. *J. Am. Chem. Soc.* **2012**, *134,* 8507–8512; Caballero, A.; White, N.G.; Beer, P.D. *Angew. Chem. Int. Ed.* **2011**, *50,* 1845–1848.
(18) Li, H.; Lu, Y.; Wu, W.; Liu, Y.; Peng, C.; Liu, H.; Zhu, W. *Phys. Chem. Chem. Phys.* **2013**, *15,* 4405–4414.
(19) Tobe, Y.; Utsumi, N.; Nagano, A.; Sonoda, M.; Naemura, K. *Tetrahedron* **2001**, *57,* 8075–8083.
(20) Frassineti, C.; Ghelli, S.; Gans, P.; Sabatini, A.; Moruzzi, M.S.; Vacca, A. *Anal. Biochem.* **1995**, *231,* 374–382.
(21) Cristau, H.-J.; Cellier, P.P.; Spindler, J.-F.; Taillefer, M. *Chem. Eur. J.* **2004**, *10,* 5607–5622.
(22) Miyaura, N.; Suzuki, A. *Chem. Rev.* **1995**, *95,* 2457–2483.
(23) Alvarez, S. *Dalton Trans.* **2013**, *42,* 8617–8636. ; For an alternative way of reporting these distances, see: Zordan, F.; Brammer, L.; Sherwood, P. *J. Am. Chem. Soc.* **2005**, *127,* 5979–5989.
(24) Berryman, O.B.; Bryantsev, V.S.; Stay, D.P.; Johnson, D.W.; Hay, B.P. *J. Am. Chem. Soc.* **2006**, *129,* 48–58.
(25) Althoff, G.; Ruiz, J.; Rodriguez, V.; Lopez, G.; Perez, J.; Janiak, C. *CrystEngComm* **2006**, *8,* 662–665.
(26) Hirose, K. *J. Inclusion Phenom. Mol. Recognit. Chem.* **2001**, *39,* 193–209.
(27) Massena, C.; Riel, A.M.S.; Neuhaus, G.F.; Decato, D.A.; Berryman, O.B. *Chem. Commun.* **2014**, *51,* 1417–1420.
(28) Feller, D. *J. Comput. Chem.* **1996**, *17,* 1571–1586.